Limnol. Oceanogr., 52(5), 2007, 1853–1864

Topographic shading and wave exposure influence morphology and ecophysiology of *Ecklonia radiata* (C. Agardh 1817) in Fiordland, New Zealand

S. R. Wing
Department of Marine Science, University of Otago, 310 Castle Street, Dunedin, New Zealand

J. J. Leichter
Scripps Institution of Oceanography, 9100 Gilman Drive, University of California at San Diego, San Diego, California 92093

C. Perrin
School of Biological Sciences, University of Wollongong, Wollongong NSW 2522, Australia

S. M. Rutger, M. H. Bowman, and C. D. Cornelisen
Department of Marine Science, University of Otago, 310 Castle Street, Dunedin, New Zealand

Abstract

Patterns in morphology, pigment concentration, and light saturation kinetics of *Ecklonia radiata* reveal great morphological and physiological variability among individuals from sites spanning strong gradients in topographic shading and wave exposure among the 14 fjords in southwestern New Zealand. Morphology of *E. radiata* varies from relatively narrow (85 ± 4.7 mm) (mean ± standard error), thick (3.2 ± 0.30 mm) blades from the well-illuminated, wave-exposed outer coast sites to wide, undulate (460 ± 36.8 mm,) and thin (0.46 ± 0.059 mm) blades from quiescent, topographically shaded inner fjord sites. Chlorophyll *a* (Chl *a*) concentration of blades (0.084–1.34 μg g^{-1} of tissue) and the ratio of fucoxanthin to Chl *a* (0.33 to 0.56) also increased along this gradient, indicating photoacclimation within the inner fjord populations. In situ measurements of light saturation kinetics indicate maximum photosynthetic rates at lower irradiance (I_{max} = 43.7 vs. 257 μmol quanta m^{-2} s^{-1}) for algae at inner fjord sites relative to well-lit outer fjord locations. Individuals exhibiting characteristically photoacclimated relative electron transfer rate curves had more deplete $\delta^{13}C$ (−13.35‰ to −22.35‰) than individuals with higher I_{max}. There was no significant association between the kelp morphology or geographic location and the observed recombinant DNA diversity of ITS sequences that would indicate the presence of two *Ecklonia* species in the fjords. *E. radiata* occupies a wide range of habitats in Fiordland and displays variability in morphology and photo-physiological responses to low light that coincide with gradients in wave exposure and topographically shaded light conditions.

The common kelp *Ecklonia radiata* (C. Agardh 1817) has a wide distribution across the wave-exposed rocky reefs of temperate Australasia, which extends into topographically shaded, quiescent waters in the inner reaches of Fiordland, southwestern New Zealand. *E. radiata* provides habitat complexity and is an important component of benthic primary production for the marine food web within the fjords (Lusseau and Wing 2006). In the New Zealand fjords the fragmented habitat structure and limitations on invertebrate larval dispersal caused by the predominant estuarine circulation have been shown to limit gene flow among basins (Sköld et al. 2003; Perrin et al. 2004). Here we investigate regional variability in morphology and photo-physiological responses of *Ecklonia* sp. within the 14 New Zealand fjords and investigate whether the observed variability in form and physiology is likely attributed to the presence of two species or to variation within the single species *E. radiata*. Adams (1994) reported extensive beds of the most common form *E. radiata* from the outer fjord habitats whereas a second species *Ecklonia brevipes* is reported to take on a wide thallus form in the inner fjord habitats. However, the status of this form as a separate species has not been fully tested. Evidence from reciprocal transplant experiments of *E. radiata* in other systems suggests that morphological plastic responses rather than genetic differences produce wide variation in form in this species (Fowler-Walker et al. 2006), similar to those observed in other Laminarians.

Macroalgae in the order Laminariales display variable morphology in response to the hydrodynamic (*e.g.*, Blanchette et al. 2002) and light environment (*e.g.*, Koehl and Alberte 1988) in addition to an array of physiological responses to limiting light conditions (*e.g.*, Lüning 1990). Morphological and physiological variability provides a mechanism for expanded niche breadth within a species

Acknowledgements

We thank M. Kasuya, R. McLeod, K. Rodgers, R. Frew, E. Serrão, M. Dowton, J. Ackerman, and two anonymous reviewers for assistance with this work. Technical support was provided from the Departments of Marine Science and Chemistry at University of Otago, Centro de Ciencias do Mar at University of Algarve, University of Wollongong, and from Scripps Institution of Oceanography and the SIO Associates. Monetary support was provided from the Royal Society of New Zealand Marsden Fund to S.R.W. (UO-00213).

(Gerard and Mann 1979), however phenotypes may represent a trade-off between photosynthetic efficiency, nutrient uptake, and structural robustness to withstand wave forces (*e.g.*, Blanchette et al. 2002). Typically kelps in wave-exposed habitats have narrow thickened blades with a corrugated surface or serrated edges, whereas algae growing in sheltered, calmer waters exhibit wider, thinner, and undulate blades (*e.g.*, Gerard and Mann 1979).

Numerous observations have been made of morphological and demographic variation in Laminarians along wave exposure gradients (*e.g.*, Rinde and Støtun 2005) with evidence for differential survivorship linked to morphology (Blanchette et al. 2002). Studies of morphological variability in algae have commonly been limited to comparisons between two distinct areas encompassing extremes of a single environmental gradient (*e.g.*, Blanchette et al. 2002). Recently, however, Miller et al. (2000) provide evidence for ecotypic divergence in macroalgae among common habitats across a region. The New Zealand fjords comprise a series of replicate basins with strong physical gradients associated with topographic shading of light by the surrounding mountains and sheltering from open coastal waves. This system provided an opportunity to resolve genotypic effects of isolation by distance from patterns in morphological and physiological variability across physical gradients.

Light limitation in kelps is known to occur because of the extinction of light with water depth (*e.g.*, Lüning 1979), self-shading (*e.g.*, Koehl and Alberte 1988), and shading under dense canopy or high stand densities (*e.g.*, Reed and Foster 1984). In the present study we investigate the effects of topographic shading on light limitation in *E. radiata*, a mechanism not previously studied. Common indications of the physiological responses to light limitation include increases in the chlorophyl *a* (Chl *a*), chlorophyl *c* (Chl *c*), and fucoxanthin content of blades in response to low light levels (Ramus et al. 1977; Wheeler 1980) and increases in the relative amounts of accessory pigments, such as fucoxanthin, in response to spectral shifts in available light (*e.g.*, Falkowski and LaRoche 1991). Typically, the initial slope of the photosynthesis–irradiance curve is steeper and the irradiance at maximum photosynthetic rate decreases in algae acclimated to low light conditions (*e.g.*, Lüning 1990).

The inorganic carbon budget of algae may also change under light-limiting conditions. At below-saturating irradiance, increases in irradiance lead to a greater demand for carbon and provide the energy required for assimilating bicarbonate, a more abundant and isotopically heavier source of carbon than dissolved CO_2 (CO_2 (aq)). Thus, algal taxa capable of assimilating bicarbonate may have elevated (heavier) $\delta^{13}C$ signatures under saturating irradiance relative to those under light-limited conditions (Kübler and Raven 1995). Under light-limiting conditions, these algae may rely more heavily on CO_2 (aq.), with this uptake reflected by $\delta^{13}C$ more depleted in ^{13}C (Kübler and Raven 1995).

We examined each of these reported variations in kelp morphology and physiological responses to light limitation as the basis for a regional description of the variability within *Ecklonia* across multiple environmental gradients. We tested the specific hypotheses that variability in kelp morphology could be statistically explained by patterns in topographic shading, depth, and wave exposure among sites, and that variability in light saturation behavior and $\delta^{13}C$ of individuals could be statistically explained by site-specific topographic shading. We also examined the genetic distinctiveness of *Ecklonia* from outer coast and inner fjord sites to test whether the observed morphological and physiological variability could be explained by the presence of two species in the fjords. The results have important implications for understanding the mechanisms that lead to broad niche breadth in kelps inhabiting complex environments such as Fiordland and in other systems such as the Chilean, Scandinavian, and British Columbian fjord systems. Fjord systems such as these comprise an important component of temperate marine environments worldwide.

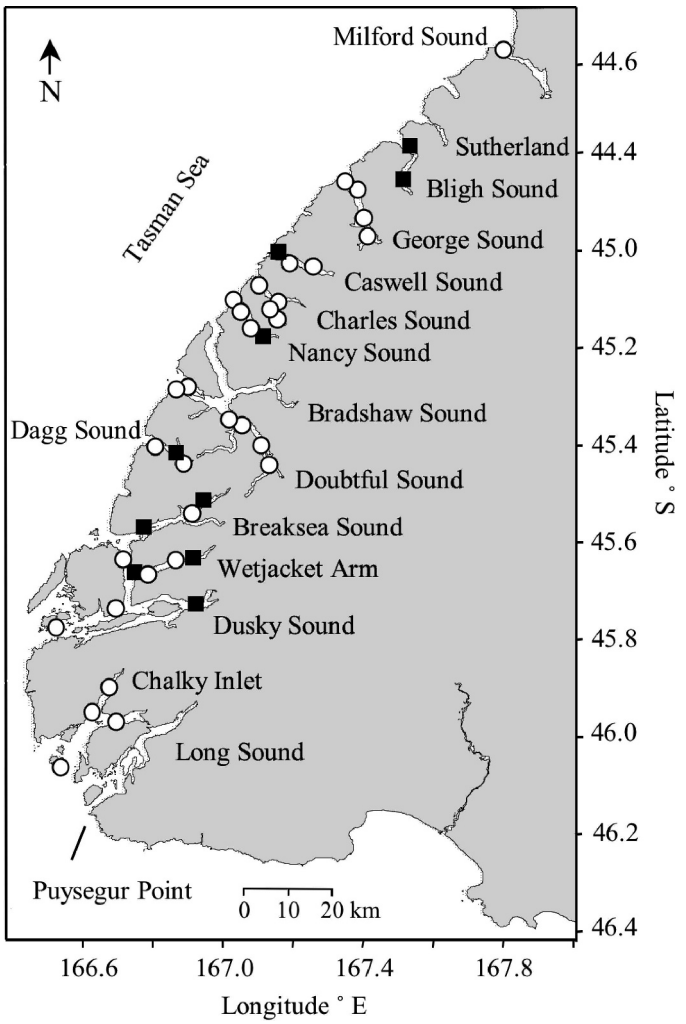

Fig. 1. A map of Fiordland with the location of study sites indicated by open circles. Closed squares indicate sources of genetic samples.

Methods

Study sites—The study was conducted in the series of 14 fjords along the southwest coast of the South Island of New Zealand at 42 semi-sheltered outer fjord and inner fjord locations (Fig. 1). Morphological data were collected at 33

sites at 10-m depth ($n = 194$) in 2002 and at 5-m, 10-m, 15-m, and 20-m depth at 18 sites in 2003 ($n = 323$), along with isotopic analysis ($n = 82$) and light saturation behavior using pulse amplitude modulated (PAM) fluorescence ($n = 94$). In 2004 a subset of nine sites were sampled at 5 m, 10 m, and 15 m for morphological information ($n = 117$), and six sites were sampled in Doubtful Sound for morphology and pigment concentration ($n = 47$).

Distance to fjord entrances—The distance from study sites to the outer coast was calculated in each fjord using a geographic information system (GIS) with 50-m horizontal resolution in the inner fjords. In this case a mean coastline raster line served as a zero line for the distance algorithm r.cost in GRASS 5.3 (Geographical Resources Analysis Support System) (ITC-irst). r.cost uses a ''knight's move'' distance calculation on a square grid to accurately provide distances around complex coastlines (Neteler and Mitasova 2002).

Regional wave exposure model—The Simulating Waves Nearshore (SWaN) (Delft University of Technology) wave model was used to produce a regional wave exposure layer for the Fiordland coastline. This model incorporated many of the important processes that lead to spatial variability in the wave climate as ocean waves approach the coastline, including shoaling, wave breaking, energy dissipation, reflection, and refraction (*e.g.*, Kirby and Dalrymple 1983; Booij et al. 2004). A detailed methodology for the SWaN wave model is given in Booij et al. (2004). Boundary conditions for the model runs were provided from a 20-yr hind-cast of regional wind and wave parameters produced by the wave analysis model (WAM) regional wave model, detailed by Gorman et al. (2003). This modeled wave climatology was forced by regional wind predictions from the European Centre for Medium Range Weather Forecasts. Gorman et al. (2003) provided a description of the regional wave model for the deepwater wave climate and a validation of the coastal wave climate.

To account for differences in the structural exposure to the wave field, the directional components of the regional wave climatology were divided into 10° bins and then combined in a weighted mean of significant wave height. Within the model the spectral directional resolution was set at 3.6° for each of the models run at 50-m resolution. The grid resolution in frequency space was set at 18 divisions of discrete frequencies for all model runs. The resulting data from these simulations were used to develop a GIS data layer for significant wave height across the fjord entrance regions.

Solar geometry model of topographic shading—Data on the mean solar irradiance in the fjords was modeled using r.sun within the GRASS GIS package (Hofierka and Suri unpubl.). In this program solar geometry and the interaction of solar radiation with the atmosphere was based on the work of Kittler and Mikler (1986) and Jenco (1992). The model considered the effect of local topography, derived from the 10-m Landcare Institute New Zealand contours, on shadow formation and computed daily sums of solar irradiance. Neteler and Mitasova (2003) provided a detailed methodology for the model. Model runs were summarized to create maps of mean annual solar irradiance in W h m^{-2} d^{-1} resolved to 50 m. For this approach atmospheric turbidity values over Fiordland were obtained for each month of the year from the Linke database obtained from www.helioclim.net.

Surface salinity—We collected salinity and temperature readings every 0.5 s from the surface to 50 m at each study site during each year using a Seabird SBE 19 conductivity, temperature, and depth profiler (CTD). Data were post-processed to 0.5-m bins using standard Seabird processing algorithms for the pumped SBE-19. Surface salinity was calculated as the mean salinity in the upper 2 m of the water column.

Morphology—In 2002, 2003, and 2004 during November, five to seven mature *E. radiata* individuals were haphazardly collected from each study site and depth (*see Study sites*) and morphological information was recorded for each individual. Frond length and width; stipe length and diameter; secondary blade number, width and length; and frond thickness at intervals of 10 cm along the length of the blade from the intercalary meristem to eroding tip were measured for each individual. Analysis of variance was used for the nine sites that were sampled in each year to test for temporal changes in morphology. The data were pooled among years in the absence of significant effects of the factor ''year'' in the model. Regression analysis was used to investigate the relationship between these pooled morphological metrics and distance from the fjord entrances among sites. This provided the basis for resolving geographic gradients in morphology among the multiple fjords.

Pigment extraction—Three replicate 1.6 cm^2 discs of tissue were collected from each *E. radiata* blade within a clean area 7–10 cm from the meristem region. Discs were immediately frozen and stored at −80°C until processing. The concentrations of pigments, including Chl *a*, chlorophyl *b*, Chl *c*, and fucoxanthin, within discs were estimated using methods described by Seeley et al. (1972) and modified by Wheeler (1980). Mean pigment concentrations from the three replicate discs were calculated for each individual. Data were expressed as g pigment per cm^2 surface area and per g wet weight of the tissue sampled. The relationships between blade thickness and Chl *a* concentration (g Chl *a* g^{-1} tissue) and the ratio of Chl *a* to fucoxanthin were tested using regression analysis. Best fit was compared between linear and non-linear models.

PAM fluorometry—In situ PAM measurements were made on intact *E. radiata* individuals using the saturation pulse method to measure relative electron transfer rate (rETR) (Schreiber et al. 1986). Light saturation curves were estimated from the relative electron transfer rates (rETR) and photosynthetically active radiation (PAR) using an underwater pulse amplitude modulated fluorometer (PAM-2000, Walz) at irradiances between 0 μmol quanta m^{-2} s^{-1}

and 550 μmol quanta m^{-2} s^{-1}. Divers sampled 3–5 individuals in situ at each depth stratum by attaching the fiber optic cable with a leaf clip to a clean area 7–10 cm from the meristem of the algal thallus on the central blade. rETR curves were collected at four or five depth ranges (2.5 to 7.5 m, 7.5 to 12.5 m, 12.5 to 17.5 m, 17.5 to 22.5 m, and 22.5 to 27.5 m) dependant on the site specific distribution of *E. radiata*. Data were collected at mid-day conditions between 10:00 h and 14:00 h at all sites. The individual algae were subsequently tagged, collected, and stored aboard the research vessel in a well-aerated aquarium before measurements of dark-adapted yield at night. The potential quantum yield of electron flow through photosystem II was measured on dark adapted algae from $F_v : F_m$, where F_m is the maximum, F_o is the value when all reaction centers are open in darkness, and $F_v = F_m - F_o$.

Each of the light saturation curves was approximated using a three-parameter model describing photosynthesis–irradiance relationships with photoinhibition from Frenette et al. (1993) where

$$P = P_s\left(1 - \exp\left(\frac{-\alpha I}{P_s}\right)\right)\left(\exp\frac{-\beta I}{P_s}\right) \quad (1)$$

P is the photosynthetic rate, I is the irradiance in μmol quanta m^{-2} s^{-1}, P_s is the maximum photosynthetic rate, α is the initial slope of the light-saturating portion of the relationship, and β is the photoinhibition parameter, which describes the negative slope in the curve at high PAR. The maximum photosynthetic rate P_{max} (i.e., maximum electron transport rate) is given by

$$P_{max} = P_s\left(\frac{\alpha}{\alpha+\beta}\right)\left(\frac{\beta}{\alpha+\beta}\right)^{\frac{\beta}{\alpha}} \quad (2)$$

The irradiance where P_{max} occurs (I_{max}) is defined as

$$I_{max} = \frac{P_s}{\alpha}\ln\left(\frac{\alpha+\beta}{\beta}\right) \quad (3)$$

The parameters of these models were approximated using non-linear fitting procedures in SAS JMP 5.1. Because of the variability in P_s with time of day and light intensity, only the parameters that describe light saturation behavior, α, and I_{max} were used to make comparisons among different plants under field conditions (Maxwell and Johnson 2000). Regression analysis was used to test the relationship between blade thickness and I_{max} among sites. Best fit was compared between linear and non-linear models.

Isotopic analysis $\delta^{13}C$ and $\delta^{15}N$—Two tissue samples were collected and frozen for storage for each alga sampled in the photosynthetic study. Samples were prepared for isotopic analysis by standard techniques. Analyses of $\delta^{13}C$ and $\delta^{15}N$ was performed on a Europa 20-20 update stable isotope mass spectrometer interfaced to a Carlo Erba elemental analyser (NA1500) in continuous flow mode (Microanalytical Laboratory, Department of Chemistry, University of Otago, precision: 0.2‰) on 1–2 mg of homogenized sample. An ethylenediamine tetraacetic acid (EDTA) laboratory standard reference was measured every six samples. This laboratory standard reference was supplied by Elemental Microanalysis and compared with international standards (IAEACH-6 for carbon, IAEAN1 and IAEAN2 for nitrogen). For these studies we accepted 0.2% accuracy in δ-values. Regression analysis was used to test the relationship between I_{max} and $\delta^{13}C$ among individuals.

General linear models—General linear models (SAS JMP 5.1) were used to test the relationship between patterns in the environmental data and models of light and wave exposure and the morphological and light saturation behavior of *E. radiata*. For those nine sites that were sampled for 3 years, the relationship between year and each morphological variable was examined. In the absence of a significant relationship the data were pooled among years and the variability across site averages was examined, but depth was retained as a variable. A model using depth (m), significant wave height (H_{sig} m), and average global irradiance (kW h m^{-2} yr^{-1}) was applied to each morphological variable for the whole data set and to I_{max} for the 2003 samples.

DNA extraction and nuclear-encoded recombinant DNA (rDNA) internal transcribed spacers sequences—Samples were collected for genetic analysis from 10 sites selected to represent the extreme range of morphological variability: Bligh Sound inner (*BLI*) and outer (BLIO, BLO), Nancy Sound inner (*NI*), Caswell Sound outer (CWO), Breaksea Sound outer (BC) and inner (*VA*), Wetjacket Arm outer (WJO) and inner (*WJI*), and Dusky inner (*GI*) and inner Dagg Sound (*OP*). Samples of *E. radiata* were also obtained from Wollongong, Eastern Australia (WOLL). Genomic DNA was extracted from dried ground algal tissue using a hexadecyltrimethylammonium bromide (CTAB) extraction method (Doyle and Doyle 1987) and following Yoon et al. (2001). Partial sequences of 26S and 18S and complete internal transcribed spacers (ITS)1, 5.8S, and ITS2 sequences were amplified by polymerase chain reaction (PCR) using the primers LB1 (5′-CGCGAGTCATCAGCTCGCATT-3′) and LB2 (5′-GCTTCACTCG CCGTACTGG-3′) (Yoon et al. 2001). Amplifications were carried out in 30-μL reaction mixtures containing about 20–200 ng *E. radiata* DNA, 0.2 mmol L^{-1} of each dNTP, 2 mmol L^{-1} $MgCl_2$, 10 mmol L^{-1} Tris-HCl (pH 8.3), 50 mmol L^{-1} KCl, 0.5 μmol L^{-1} of each primer, and 0.25 unit of *Taq* DNA polymerase (Biocat). The PCR regime consisted of one cycle of denaturation at 94°C for 5 min followed by 35 cycles of 1 min at 94°C, 1 min at 53°C, and 1 min at 72°C and finished by a final elongation of 4 min at 72°C using a PTC-100 thermal cycler (Applied Biosystems). PCR products were sent for cycle sequencing with both primers LB1 and LB2 (Macrogen) to obtain the complete sequence of the ITS1 and ITS2 regions. The electropherograms for each sample were checked visually using Bioedit. Previously published sequences of *E. radiata* from Whitfords Reef, Western Australia (Lane et al. 2006), *E. cava* Kjellman, *E. stolonifera* Okamura, *Eckloniopsis*

radicosa (Kjellm.) Okamura (Yoon et al. 2001), and *Eisenia bicyclis* (Kjellm.) Setchell (Yoon and Boo 1999) were included in the analysis. Nuclear rDNA ITS are relatively fast-evolving and have previously permitted the distinction between closely related species, including brown algae (Druehl et al. 1997; Peters et al. 1997; Serrão et al. 1999; Yoon et al. 2001; Lane et al. 2006). ITS sequence variation was thus used to compare levels of genetic variation between the two morphological groups of *Ecklonia radiata* inhabiting the fjords to the genetic divergence observed within the species between distant regions (Fiordland-Australia) to determine whether the variability observed in the fjords can be attributed to the presence of two separate species. The phylogenetic tree was rooted with the outgroup sequence of a species belonging to the same family *E. bicyclis* (Yoon et al. 2001). Other related species of the same family (e.g., *E. cava, E. stolonifera, E. radicosa*, and *E. bicyclis*, Yoon et al. 2001) were added in the analysis, and their presence was used for comparison of intraspecific difference within the potential *E. radiata* species complex within the fjords versus interspecies divergences. The sequences contained between the primers LB1 and LB2 were aligned using CLUSTALW implemented in Bioedit and improved manually. The total alignment was 1007-bp long including insertions/deletions (indels) (ITS 1 318 bp, ITS 2 378 bp). Each of the sequences was submitted to Genbank (accession numbers DQ662103–DQ662133).

Phylogenetic analyses—Best-fit models of sequence evolution were selected for partitioned regions of DNA (ITS2, ITS1 separately) from 24 different models of sequence evolution implemented in PAUP* 4.0b10 (Swofford 1998) using hierarchical likelihood ratio tests in the program MrModeltest 2.2 (Nylander 2004). Indels (insertions/deletions) were treated as missing data. 26S, 5.8S, and 18S were invariable, therefore no model was selected in the best-fit model analysis. The F81 model (Felsenstein 1981) showed the highest likelihood score for the model of sequence evolution of ITS2, and JC (Jukes and Cantor 1969) was the best-fit model for the sequence evolution of ITS1. Bayesian phylogenetic analyses of partitioned data were performed using MrBayes 3.1 (Huelsenbeck and Ronquist 2003; Ronquist et al. 2005) using the previously selected models of sequence evolution. Indels did not contribute any phylogenetic information in the Bayesian analysis. In order to use the information in the indels, these events were coded as binary characters (presence/absence of gaps) and included as a separate binary data partition in our analysis (Ronquist et al. 2005). Trees were rooted with the outgroup sequence of *E. bicyclis*. The Markov chain Monte Carlo search (mcmc) was run for 5,000,000 generations, with four chains, trees being sampled every 100 generations after the first 12,500. Final average standard deviations of split frequencies were below 0.01, indicating that the runs had reached stationarity. Analyses were repeated to ensure that independent runs converged on similar topologies. Net mean sequence divergences among groups of samples ($dxy - 0.5(dx + dy)$, Nei 1987) were calculated using the software Arlequin Version 3.0 (Excoffier et al 2005), incorporating the JC distance matrix among sequences and pairwise difference for restriction fragment length polymorphism (RFLP)-type data for indels information.

Results

SWaN wave model—The gradients in wave exposure in New Zealand fjords were extremely sharp. Open ocean swells as large as 2–9 m occurred regularly on the exposed coast and fjord entrances, while entirely sheltered waters existed within the inner portions of the fjords. In many of the fjords the penetration of wave energy into the entrances was highly dependant on the distribution of swell direction. For example, some of the northern fjords (Nancy, Caswell Sounds) had a northerly aspect to the entrance sill, and they were completely sheltered from the dominant swell direction (SW). In some of the southern fjords (e.g., Chalky Inlet), exposure to the southwest resulted in wave energy propagation into the inner reaches of the fjords. Several of the fjords with complex island systems at the entrances (Doubtful, Breaksea, Dusky, Preservation) displayed the sheltering effects of the islands. These data were useful for understanding the mean wave conditions in the fjord entrances (Table 1).

Topographic shading—Results from the r.sun model indicated that the yearly sum of irradiance (kW h m^{-2} yr^{-1}) from direct and diffuse sources was variable among sites (Table 1). Values ranged between 2,123 kW h m^{-2} yr^{-1} and 1,035 kW h m^{-2} yr^{-1} among individual sites. Much of this variability could be attributed to the direct component of irradiance and to topographic shading by mountains at the south-facing study sites in the inner fjords. These data were used to test the contribution of irradiance in the regional statistical model of morphological variability and to test the specific effect of irradiance on light saturation behavior in algae among sites.

Surface salinity—Large variation in the surface salinity was evident among fjords (Table 1). The inner regions of Doubtful Sound differed from all the other regions, showing lower surface salinity associated with the outflow of freshwater from the Manapouri hydroelectric power plant. Surface salinity is an effective predictor of the depth of the low salinity layer among sites, which has been demonstrated to influence the subtidal light environment (Goebel et al. 2005). In this case dissolved tannins and organic material result in both increased light extinction and spectral shifts in irradiance. Surface salinity data were, therefore, used in the regional statistical model of morphological variability in *E. radiata*.

Morphology—E. radiata morphology was distributed continuously from relatively narrow (85 ± 5 mm) (mean ± SE) and thick (3.2 ± 0.3 mm) blades at sites on the outer coast to wide, undulate (460 ± 37 mm,) and thin (0.46 ± 0.06 mm) blades at sites in the inner fjords ($n = 681$). This

Table 1. Environmental variables for each of the study sites.

Fjord	Site	Distance (km)	Salinity	Irradiance (kW h m^{-2} s^{-1})	H_{sig} (m)
Milford	1	0.13	32.91	2,123	0.767
Bligh	2	12.28	30.76	1,564	0.030
	3	5.16	32.65	1,835	0.206
George	4	15.05	31.88	1,934	0.028
	5	11.67	32.20	1,891	0.127
	6	4.7	33.05	1,666	0.439
	7	1.62	33.26	1,872	0.605
Caswell	8	7.53	31.62	1,855	0.172
	9	3.92	29.47	2,082	0.158
	10	1.99	30.08	1,912	0.120
Charles	11	10.28	31.77	1,894	0.007
	12	7.33	31.29	2,029	0.139
	13	7.16	31.28	2,031	0.162
	14	2.83	32.41	1,961	0.139
Nancy	15	11.28	33.07	1,981	0.056
	16	6.27	33.25	1,919	0.120
	17	1.86	33.33	2,037	0.343
	18	0.15	33.43	1,915	0.429
Doubtful	19	29.01	14.41	1,866	0.010
	20	24.78	16.50	1,841	0.016
	21	17.51	19.88	2,051	0.120
	22	16.21	19.23	2,048	0.150
	23	4.08	23.12	2,061	0.295
	24	4.62	22.83	2,051	0.337
Dagg	25	9.13	32.35	1,796	0.158
	26	7.58	32.61	1,972	0.173
	27	3.24	32.90	2,053	0.355
Breaksea	28	23.39	29.07	1,035	0.020
	29	20.73	29.49	1,922	0.040
	30	10.16	31.04	1,515	0.271
	31	8.52	30.91	1,859	0.131
Wetjacket	32	25.7	28.86	1,641	0.010
	33	21.27	30.58	1,161	0.020
	34	15.06	29.02	2,005	0.169
	35	13.01	30.57	2,004	0.147
Dusky	36	36.05	23.69	2,029	0.020
	37	20.64	29.48	1,692	0.130
	38	7	29.79	1,828	0.169
Chalky	39	19.61	31.03	1,941	0.591
	40	14.95	32.10	1,987	0.306
	41	16.78	32.36	2,072	0.214
	42	0.12	33.97	1,972	0.786

was apparent from the relationships between blade width (Fig. 2a), blade thickness (Fig. 2b), blade length (Fig. 2c), and distance to the fjord entrances.

Regression analysis between site averages ($n = 42$) of each of the morphological variables and distance to the outer coast followed a significant linear relationship (blade width (mm) = (107 ± 16) + (10 ± 1) distance (km), $p < 0.0001$, $r^2 = 0.65$, $n = 42$; blade thickness (mm) = (2 ± 0.1) − (0.06 ± 0.01) distance (km), $p < 0.0001$, $r^2 = 0.56$, $n = 42$; blade length (mm) = (278 ± 32) + (16 ± 2) distance (km), $p < 0.0001$, $r^2 = 0.57$, $n = 42$).

Pigment analysis—Along this same gradient from outer coast to inner fjord sites there was an increase in Chl *a* concentration (0.084 μg g^{-1} tissue to 1.34 μg g^{-1} tissue) and an increase in the ratio of fucoxanthin to Chl *a* (0.33 to 0.56) ($n = 236$). The relationship between mean Chl *a* concentration at each depth stratum and blade thickness in mm formed a significant power function (Chl a = 0.00038 thickness $^{-0.77}$, $p < 0.001$, $r^2 = 0.68$, $n = 57$) (Fig. 3a). The relationship between thickness and the ratio of Chl *a* to fucoxanthin was significant (Chl *a*/fucoxanthin = (0.52 ± 0.01) − (0.043 ± 0.004) thickness (mm), $p < 0.0001$, $r^2 = 0.68$, $n = 57$) (Fig. 3b).

PAM fluorescence—In situ measurements of light saturation kinetics indicated maximum photosynthetic rates at lower irradiance (I_{max} = 43.7 μmol quanta m^{-2} s^{-1}) for algae at inner fjord sites relative to well-lit outer fjord locations (I_{max} = 257 μmol quanta m^{-2} s^{-1}) ($n = 94$). Individuals exhibiting these low values for I_{max} also had a steeper initial slope to the rETR curve ($\alpha = 0.184$) relative

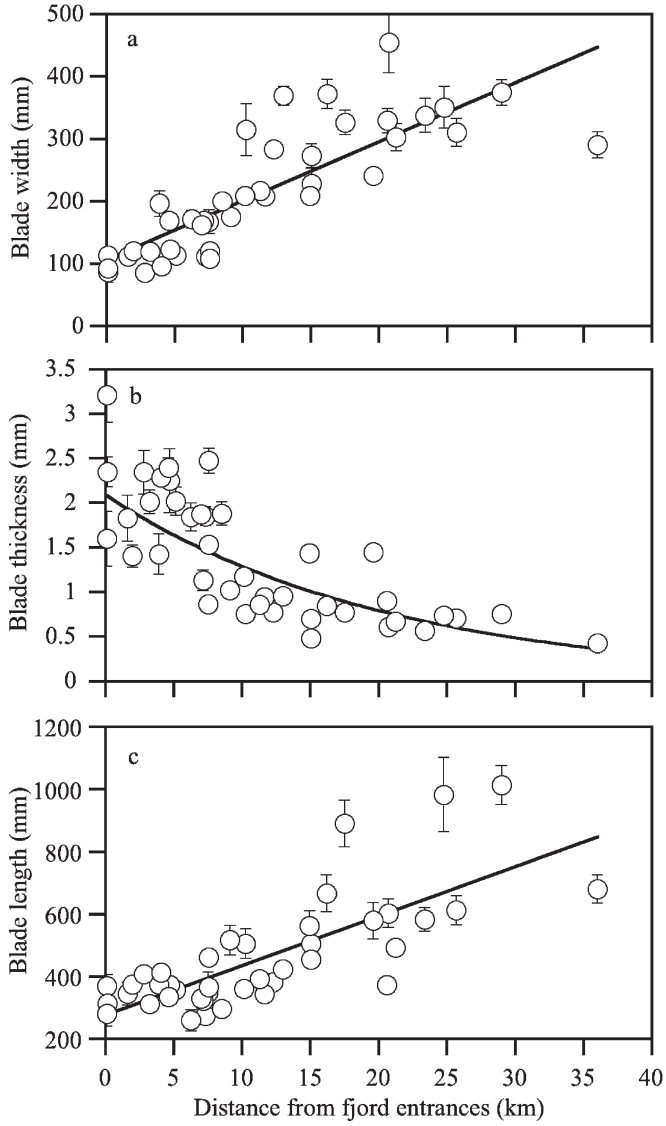

Fig. 2. Site averages of (a) blade width (mm), (b) blade thickness (mm), and (c) blade length versus distance from fjord entrance (km) for the 10–15-m depth stratum. Error bars indicate 1 SE.

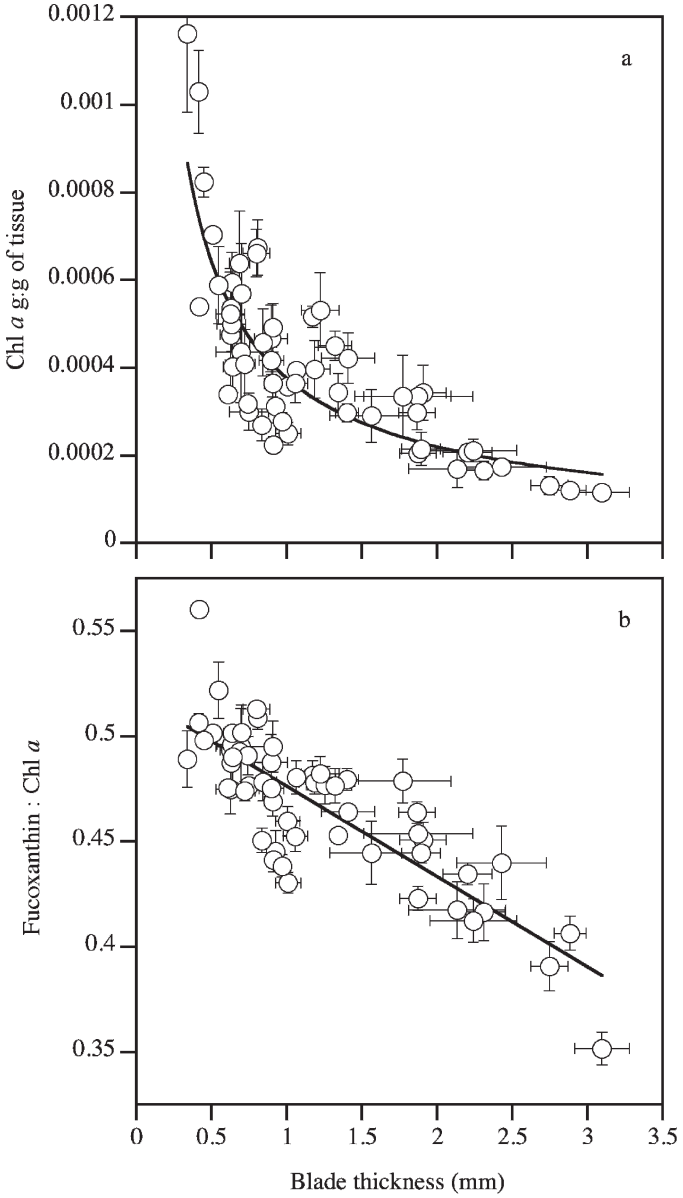

Fig. 3. Pigment concentration versus blade thickness (a) Chl *a* (g : g of tissue), and (b) the ratio between fucoxanthin and Chl *a*.

to individuals with higher I_{max} ($\alpha = 0.433$). The relationship between average blade thickness in mm and average I_{max} among depth strata formed a significant logarithmic relationship (I_{max} [μmol quanta m^{-2} s^{-1}] = 111 + 185 log[thickness], $p < 0.001$, $r^2 = 0.49$, $n = 39$) (Fig. 4a).

Isotopic analysis $\delta^{13}C$ and $\delta^{15}N$—Individuals exhibiting these characteristically photoacclimated rETR curves also had more depleted $\delta^{13}C$ (−13.35‰ to −22.35‰) than individuals with higher I_{max}. The relationship between I_{max} and $\delta^{13}C$ of individuals forms a significant linear relationship ($\delta^{13}C = (-24.39 \pm 1.60) + (0.07274 \pm 0.012)$ I_{max} (μmol quanta m^{-2} s^{-1}), $p < 0.001$, $r^2 = 0.59$, $n = 24$) (Fig. 4b). There were no clear trends in the $\delta^{15}N$ signatures.

General linear models—A general linear model of blade thickness (mm) versus depth (m), significant wave height (m), salinity, and irradiance (kW h m^{-2} yr^{-1}) indicated that 60% of the variability in blade thickness among sites could be statistically explained by the environmental variables (Table 2). Observed and predicted values of blade thickness for this model were plotted in Fig. 5a.

A general linear model of the natural log of I_{max} average irradiance (kW h m^{-2} yr^{-1}) indicated that 84% of the variance in I_{max} among individuals could be accounted for by the variation in the average irradiance (Fig. 5b) (ln I_{max} [μmol quanta m^{-2} s^{-1}] = [−0.023 ± 0.35] + [0.003 ± 0.0002] irradiance [kW h m^{-2} yr^{-1}], $p < 0.0001$, $r^2 = 0.84$, $n = 33$) and that the remaining environmental variables did not add to the predictive value of the model.

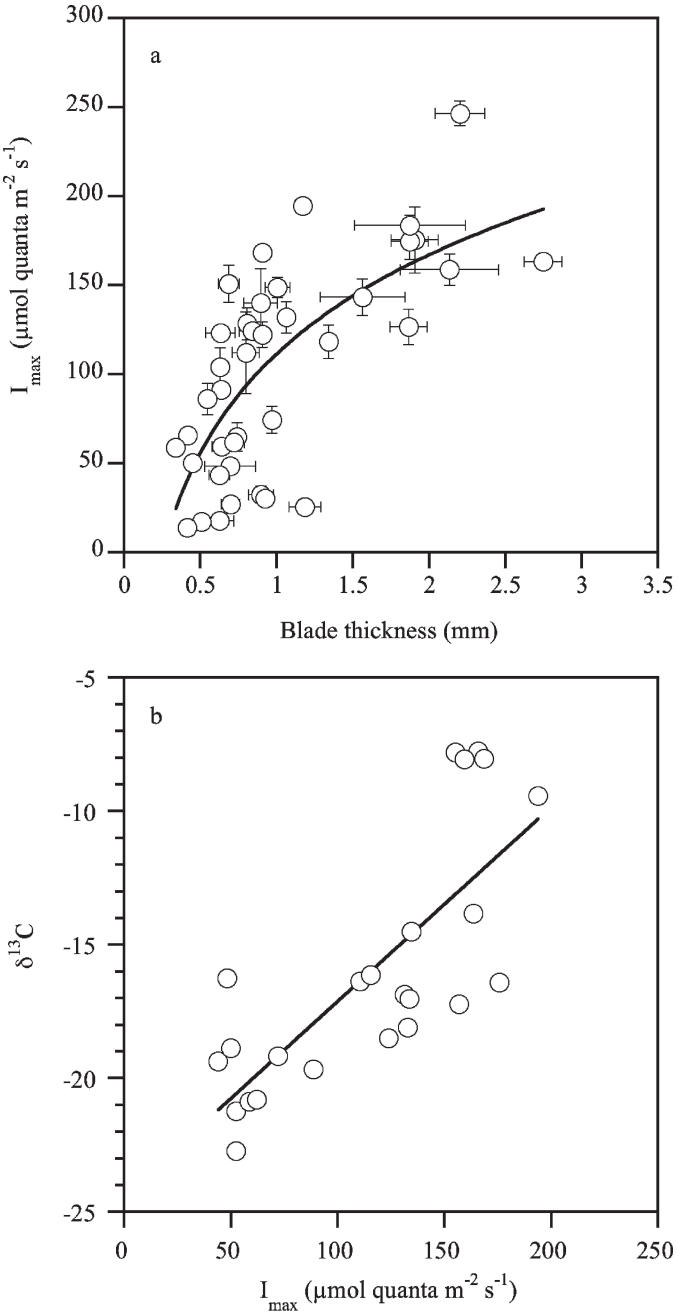

Fig. 4. Relationship between (a) irradiance at maximum electron transfer rate (I_{max}) and blade thickness and (b) irradiance at maximum electron transfer rate (I_{max}) and $\delta^{13}C$.

Table 2. General linear model of blade thickness (mm) among sites and depths versus environmental data (Fig. 5a). Summary of fit: $r^2 = 0.60$, RMSE = 0.452, $p < 0.0001$, $n = 75$.

Term	Estimate	SE	t ratio	Prob > |t|
Intercept	−2.38	0.998	−2.39	0.0198
Depth (m)	−0.0355	0.00938	−3.79	0.0003
H_{sig} (m)	4.17	0.678	6.15	<0.0001
Salinity	0.0215	0.0146	1.47	0.1451
Irradiance (kW h m^{-2} yr^{-1})	1.47 e^{-3}	4.41e^{-4}	3.33	0.0014

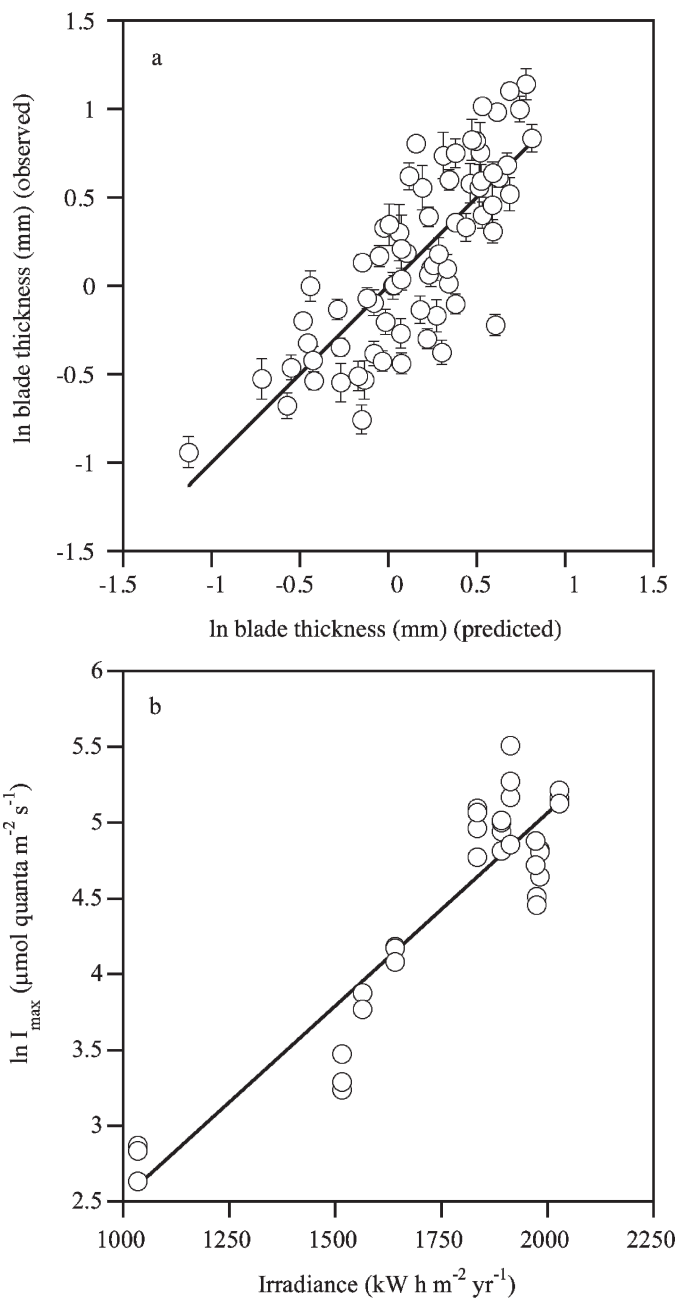

Fig. 5. Relationship between (a) observed blade thickness (mm) and predictions of the general linear model based on environmental data (Table 2), and (b) relationship between ln irradiance at maximum electron transfer rate (I_{max} µmol quanta m^{-2} s^{-1}) and irradiance (kW h m^{-2} yr^{-1}) from solar model.

Phylogenetic analyses of rDNA ITS sequences—The 31 *E. radiata* samples analyzed yielded 10 distinct sequences (Genbank accession numbers: DQ662103–DQ662133), included eight distinct sequences (A–H) among fjord sites (outer sites, four distinct sequences [$n = 9$]; inner sites, six distinct sequences [$n = 19$]) (Fig. 6). Two sequences were shared across inner and outer sites, two sequences were found at outer coast sites in more than one fjord, and two sequences were found at inner sites in more than one fjord. The Bayesian tree, which indicates genetic similarity among

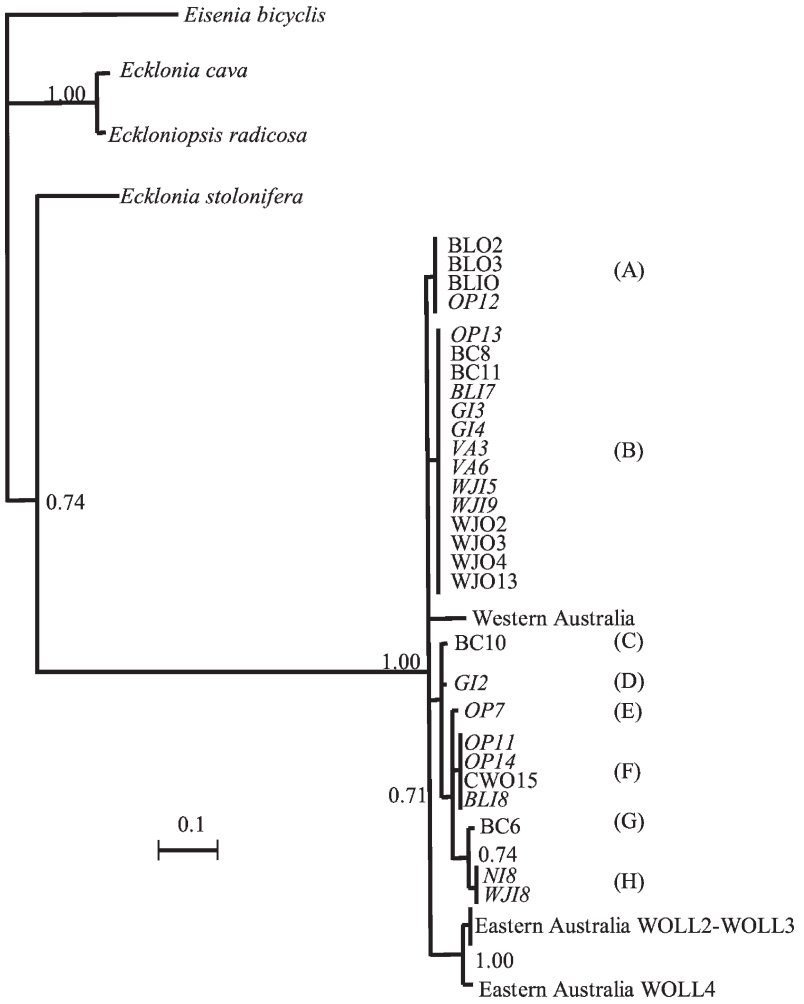

Fig. 6. Bayesian phylogenetic analysis of *Ecklonia radiata* ITS1 and ITS2 regions. Posterior probability values above 0.70 are indicated on associated nodes. Fiordland samples are from Bligh Sound inner (*BLI*) and outer (BLO), Nancy Sound inner (*NI*), Caswell Sound outer (CWO), Breaksea Sound outer (BC) and inner (*VA*), Wetjacket Arm outer (WJO) and inner (*WJI*), Dusky Inner (*GI*), and inner Dagg Sound (*OP*) (Fig. 1). Sequences of individuals with relatively wide and thin blades from sites in the inner regions of the fjords are in italics. Each of the unique sequences from the Fiordland samples is designated a label A–H on the phylogenetic tree.

groups, strongly supported the monophyly of *E. radiata* sequences from the New Zealand fjords and Australia (posterior pb 1.00), and *E. radiata* sequences were highly divergent from other *Ecklonia* species analyzed in our study. The mean net sequence divergence between the two morphological and physiological types was less than the mean net sequence divergences observed at the within-species level among geographically distant locations of *E. radiata* (Fiordland morphs, eastern and western Australia) for both values estimated from sequence and indel data (data not shown). Although there was evidence for distinct clades within the Fiordland samples, sequences did not cluster according to morphological or physiological type or to geographic location for the observed phylogenetic structure within *E. radiata*. This pattern would reflect reproduction isolation between two morphotypes. Additionally, mean net sequence divergences among potential sequence clades in the fjords were less than the sequence divergences observed among fjords and Australian samples. Thus, although our data could not exclude the possibility of within species population differentiation among *E. radiata* fjord samples or extensive hybridization between two closely related species, it appears unlikely the samples of *E. radiata* from the fjords correspond to two species, e.g., *E. radiata* and *E. brevipes* (Fig. 6).

Discussion

The results of this study provide strong support for the idea that the morphological and physiological patterns observed in *E. radiata* across a wide range of habitats in Fiordland represents variability within a single species

rather than genetic divergence between two different species. Each of the measured indicators of morphological and physiological variability form continuous distributions across environmental gradients, particularly wave exposure and irradiance. Genetic variation of *E. radiata* among samples from the fjords is less than the variation observed among geographically distant locations. The physiological variables, pigment concentration and light saturation kenetics correlate with blade thickness, a primary indicator of morphology. These patterns indicate that morphology and physiological variability in *E. radiata* are closely linked in the photoacclimation response.

Plasticity of the photosynthetic apparatus in macroalgae enables individuals to acclimate to changes in the light environment and to occupy a broad range of habitats (Ramus et al. 1976; Lüning 1990). Acclimation takes place on several different levels and includes changes in overall as well as relative pigment concentrations, and changes in the number of reaction centers as well as in thylakoid surface area and chloroplast volume (*e.g.*, Henley and Ramus 1989). Changes in pigment concentrations take place in response to changes in light quantity (intensity adaptation) as well as quality as the spectral composition of light changes with depth (chromatic adaptation) (Ramus et al. 1976). These changes result in a more efficient capture of photons, an essential adaptation for survival during the dark period of the year (Dunton and Jodwalis 1988). Changes in the photosynthetic apparatus can be observed over seasons as well as among depths with a general increase in pigment concentrations in winter and at deeper depths (Ramus et al. 1976; Wheeler 1980). The light-harvesting efficiency of an alga is also linked with its morphology. For example, thin plants appear to be more efficient than thick ones because of a greater surface area to volume ratio as well as a minimal self-shading of light-harvesting cell components (Lüning and Dring 1985). Changes in morphology, resulting in increases in the light-harvesting capacity and efficiency, are thus part of the photoacclimation response of macroalgae (Markager and Sand-Jensen 1992; Miller et al. 2006).

In brown algae the concentrations of Chl *a* and the accessory pigments Chl *c* and fucoxanthin tend to increase with depth and shading, with the greatest increases observed in Chl *a* and fucoxanthin (Ramus et al. 1977; Wheeler 1980). *E. radiata* have a stronger photoacclimative response to low light conditions than other macroalgae in subtidal kelp forests in temperate Australia (Fairhead and Cheshire 2004). Our findings show that *E. radiata* from topographically shaded and wave sheltered areas have much greater concentrations of Chl *a* and fucoxanthin, lower irradiance at maximum electron transfer rate (I_{max}), and much thinner and broader primary and secondary blades than individuals from outer fjord habitats. Thus, there is a strong photoacclimation response to the local environmental conditions in Fiordland, including both topographic shading and wave exposure.

Although the results of our regional statistical model indicate the climatological correlates for variation in morphology and photoacclimation responses of *E. radiata* among sites, there are several important caveats to interpreting the observed patterns. Potentially important factors such as stand density, grazing, and interspecific competition were not resolved in the present study. The results are limited to conclusions from regional statistical models but do not incorporate temporal variability in irradiance or wave climate. There is, in fact, pronounced seasonal variability in the light climate that may have important consequences for photoacclimation of *E. radiata* and were not resolved by the irradiance model. There is also pronounced weather-band (weekly) variability in the wave climate and seasonal variability in the frequency of storm events, which was not resolved by the climatological wave exposure model. Nevertheless, variation in these regional averages for the environmental conditions provided the basis for statistically explaining 60% of the variation in morphology and 84% of the variation in light saturation kinetics as indicated by variance in I_{max}. These models provide a good approximation of relative climatological conditions among sites because of the intense spatial variability in both light and wave exposure in the Fiordland region (Cornelisen et al. 2007).

We examined patterns in morphology relative to among site variability in nuclear-encoded rDNA ITS sequences as a basis for examining the relationships between geography, morphology, and genetic distinctiveness at the species level. Results indicated that there was no clear basis in morphological or geographic differences for rDNA diversity, and no evidence of a second cryptic species based on the sequences analyzed. In Fiordland, Nelson et al. (2002) report abundant specimens of the common kelp *E. radiata* (C. Agardh 1817) and a second species *E. brevipes* (C. Agardh 1877), although it is noted in Adams (1994) that "colonies of *E. brevipes* might develop from detached, sunken plants of 'normal' *Ecklonia* in areas with little illumination and water movement." *E. brevipes* is distinguished as having a very spreading growth form with wide-thin blades, secondary haptera along the blade margin, and an absent or very reduced stipe and holdfast. Whereas the data presented here do not refute the existence of *E. brevipes* as a separate species, they do support the supposition that *E. radiata* exists as a single species across a wide geographic and morphological range within the fjords. Further, the data suggest that *E. brevipes* could in fact be a morphological variant of *E. radiata*.

Because Fiordland consists of a series of 14 fjords, each with a gradient in wave exposure and topographic shading, we were able to sample geographically isolated sites across the full range of environmental conditions in the region independent of major changes in latitude. Rocky reef habitat in Fiordland has an unusually large range of incident irradiance because of the light-scattering characteristics of the low salinity layer (Goebel et al. 2005) and from topographic shading from the surrounding mountains. The effect of topographic shading is a novel mechanism for light limitation in benthic macroalgae, and our results indicate that it is likely the largest driver of variability in light saturation kinetics for *E. radiata* observed in this system, whereas morphology was primarily correlated with wave exposure. We observe that photoacclimation to these conditions consisted of a coupled

morphological and physiological response leading to extreme ecological variability within the species, which coincides with a wide distribution among habitats. These findings are potentially important for understanding the mechanisms influencing distribution of kelps and benthic productivity in other fjordic systems where topographic shading likely plays an important role in the light environment.

References

Adams, N. M. 1994. Seaweeds of New Zealand: An illustrated guide. Canterbury Univ. Press.

Blanchette, C. A., B. G. Miner, and S. D. Gaines. 2002. Geographic variability in form, size and survival of *Egregia menziesii* around Point Conception, California. Mar. Ecol. Progr. **239:** 69–82.

Booij, N., I. J. G. Haagsma, L. H. Holthuijsen, A. T. M. M. Kieftenburg, R. C. Ris, A. Jvan der Westhuysen, and M. Zijlema. 2004. SWaN cycle III version 40.41 user manual. Delft Univ. of Technology.

Cornelisen, C. D., S. R. Wing, K. L. Clark, M. H. Bowman, R. D. Frew, and C. L. Hurd. 2007. Patterns of macroalgal stable carbon and nitrogen isotope signatures: Interaction between physical gradients and nutrient source pools. Limnol. Oceanogr. **52:** 820–832.

Druehl, L. D., C. Mayes, I. H. Tan, and G. W. Saunders. 1997. Molecular and morphological phylogenies of kelp and associated brown algae. p. 221–235. *In* D. Bhaltacharya [ed.], Origins of algae and their plastids. Springer-Verlag.

Dunton, K. H., and C. M. Jodwalis. 1988. Photosynthetic performance of *Laminaria solidungula* measured *in situ* in the Alaskan High Arctic. Mar. Biol. **98:** 277–285.

Excoffier, L., G. Laval, and S. Schneider. 2005. Arlequin ver. 3.0: An integrated software package for population genetics data analysis. Evolutionary Bioinformatics Online **1:** 47–50.

Fairhead, V. A., and A. C. Cheshire. 2004. Seasonal and depth related variation in the photosynthesis-irradiance response of *Ecklonia radiata* (Phaeophyta, Laminariales) at West Island, South Australia. Mar. Biol. **145:** 415–426.

Falkowski, P. G., and J. LaRoche. 1991. Acclimation to spectral irradiance in algae. J. Phycol. **27:** 8–14.

Felsenstein, J. 1981. Evolutionary trees from DNA sequences: A maximum likelihood approach. J. Mol. Evol. **17:** 368–376.

Fowler-Walker, M. J., T. Wernberg, and S. D. Connell. 2006. Differences in kelp morphology between wave sheltered and exposed localities: Morphologically plastic or fixed traits? Mar. Biol. **148:** 755–767.

Frenette, J. J., S. Demers, L. Legendre, and J. Dodson. 1993. Lack of agreement among models for estimating the photosynthetic parameters. Limnol. Oceanogr. **38:** 679–687.

Gerard, V. A., and K. H. Mann. 1979. Growth and production of *Laminaria longicruris* (Phaeophyta) population exposed to different intensities of water movement. J. Phycol. **15:** 33–41.

Goebel, N. L., S. R. Wing, and P. W. Boyd. 2005. A mechanism for onset of diatom blooms in a fjord with persistent salinity stratification. Estuar. Coast. Shelf Sci. **64:** 546–560.

Gorman, R. M., K. R. Bryan, and A. K. Laing. 2003. A wave hind-cast for the New Zealand region—nearshore validation and coastal wave climate. New Zeal. J. Mar. Freshwat. Res. **37:** 567–588.

Henley, W. J., and J. Ramus. 1989. Optimization of pigment content and the limits of photoacclimation for *Ulva rotundata* (Chlorophyta). Mar. Biol. **103:** 267–274.

Huelsenbeck, J. P., and F. Ronquist. 2001. MrBayes: Bayesian inference of phylogeny. Biometrics **17:** 754–755.

Jenco, M. 1992. Distribution of direct solar radiation on georelief and its modelling by means of complex digital model of terrain. Geograficky casopis **44:** 342–355.

Jukes, T., and C. Cantor. 1969. Evolution of protein molecules. p. 21–132. *In* H. N. Munro [ed.], Mammalian protein metabolism. Academic Press.

Kirby, J. T., and R. A. Dalrymple. 1983. A parabolic equation for the combined refraction-diffraction of Stokes waves by mildly varying topography. J. Fluid Mech. **136:** 543–566.

Kittler, R., and J. Mikler. 1986. Basis of the utilization of solar radiation. VEDA, Bratislava.

Koehl, M. A. R., and R. S. Alberte. 1988. Flow, flapping and photosynthesis of *Nereocystis luetkeana*: A functional comparison of undulate and flat blade morphologies. Mar. Biol. **99:** 435–444.

Kübler, J. E., and J. A. Raven. 1995. The interaction between inorganic carbon acquisition and light supply in *Palmaria palmata* (Rhodophyta). J. Phycol. **31:** 369–375.

Lane, C. E., C. Mayes, L. D. Druehl, and G. W. Saunders. 2006. A multi-gene molecular investigation of the kelp (Laminariales, Phaeophyceae) supports substantial taxonomic re-organization. J. Phycol. **42:** 493–512.

Lüning, K. 1979. Growth strategies of three *Laminaria* species (Phaeophyceae) inhabiting different depth zones in the sublittoral region of Helgoland (North Sea). Mar. Ecol. Progr. **1:** 195–207.

———. 1990. Seaweeds: Their environment, biogeography and ecophysiology. Wiley.

———, and M. J. Dring. 1985. Action spectra and spectral quantum yield of photosynthesis in marine macroalgae with thin and thick thalli. Mar. Biol. **87:** 119–129.

Lusseau, S. M., and S. R. Wing. 2006. Importance of pelagic subsidies versus local production to the diet of a closed population of bottlenose dolphins (*Tursiops sp.*). Mar. Ecol. Progr. **321:** 283–293.

Markager, S., and K. Sand-Jensen. 1992. Light requirements and depth zonation of marine macroalgae. Mar. Ecol. Progr. **88:** 83–92.

Maxwell, K., and G. N. Johnson. 2000. Chlorophyll fluorescence—a practical guide. J. Exp. Bot. **51:** 659–668.

Miller, S. M., S. R. Wing, and C. L. Hurd. 2006. Photoacclimation of *Ecklonia radiata* (Laminariales, Heterokontophyta) in Doubtful Sound, Fjordland, Southern New Zealand. Phycologia **45:** 44–52.

Miller, K. A., J. L. Olsen, and W. T. Stam. 2000. Genetic divergence correlates with morphological and ecological subdivision in the deep-water elk kelp *Pelagophycus porra* (Phaeophyceae). J. Phycol. **36:** 862–870.

Nei, M. 1987. Molecular evolutionary genetics. Columbia Univ. Press.

Nelson, W. A., E. Villouta, K. F. Neill, G. C. Williams, N. M. Adams, and R. Slivsgaard. 2002. Marine macroalgae of Fiordland, New Zealand. Tuhinga **13:** 117–152.

Neteler, M., and H. Mitasova. 2002. Open source GIS: A GRASS GIS approach. Kluwer.

Nylander, J., F. Ronquist, J. Huelsenbeck, and J. Nieves-Aldrey. 2004. Bayesian phylogenetic analysis of combined data. Syst. Biol. **53:** 47–67.

Perrin, C., S. R. Wing, and M. S. Roy. 2004. Population genetic structure amongst populations of the sea star *Coscinasterias muricata* in the New Zealand fjords. Mol. Ecol. **13:** 2183–2195.

Peters, A. F., M. J. H. vanOppen, C. Wiencke, W. T. Stam, and J. L. Olsen. 1997. Phylogeny and historical ecology of the Desmarestiaceae (Phaeophyceae) support a southern hemisphere origin. J. Phycol. **33:** 294–309.

Ramus, J., S. I. Beale, D. Mauzerall, and K. L. Howard. 1976. Changes in photosynthetic pigment concentration in seaweeds as a function of water depth. Mar. Biol. **37:** 223–229.

———, F. Lemons, and C. Zimmerman. 1977. Adaptation of light-harvesting pigments to downwelling light and the consequent photosynthetic performance of the eulittoral rockweeds *Ascophyllum nodosum* and *Fucus vesiculosus*. Mar. Biol. **42:** 293–303.

Reed, D. C., and M. Foster. 1984. The effects of canopy shading on algal recruitment and growth in a giant kelp (*Macrocystis pyrifera*) forest. Ecology **65:** 937–948.

Rinde, E., and K. Sjøtun. 2005. Demographic variation in the kelp *Laminaria hyperborean* along a latitudinal gradient. Mar. Biol. **146:** 1051–1062.

Ronquist, F., J. Huelsenbeck, and P. van der Mark. 2005. MrBayes 3.1 manual.

Schreiber, U., U. Schliwa, and W. Bilger. 1986. Continuous recording of photochemical and non-photochemical chlorophyll fluorescence quenching with a new type of modulation fluorometer. Photosynth. Res. **10:** 51–62.

Serrão, E. A., L. A. Alice, and S. H. Brawley. 1999. Evolution of the Fucaceae (Phaeophyceae) inferred from nrDNA- ITS. J. Phycol. **35:** 382–394.

Sköld, M., S. R. Wing, and P. V. Mladenov. 2003. Genetic subdivision of the sea star *Coscinasterias muricata* in the fjords of New Zealand. Mar. Ecol. Progr. **250:** 163–174.

Swofford, D. L. 2001. PAUP: phylogenetic analysis using parsimony (and other methods). V.4.0b8. Sinauer.

Wheeler, W. N. 1980. Pigment content and photosynthetic rate of the fronds of *Macrocystis pyrifera*. Mar. Biol. **56:** 97–102.

Yoon, H. S., and S. M. Boo. 1999. Phylogeny of Alariaceae (Phaeophyta) with special reference to *Undaria* based on sequences of the RuBisCo spacer region. Hydrobiologia **398/399:** 47–55.

———, J. Y. Lee, S. M. Boo, and D. Bhattacharya. 2001. Phylogeny of Alariaceae, Laminariaceae, and Lessoniaceae (Phyaeophyceae) based on plastid-encoded RuBisCo spacer and nuclear-encoded ITS sequences comparisons. Mol. Phylogenet. Evol. **21:** 231–243.

Received: 26 December 2006
Accepted: 9 May 2007
Amended: 22 May 2007